

Investigations of $\eta \rightarrow \pi^0 \gamma \gamma$

ANKHI ROY for CBELSA TAPS Collaboration

Department of Physics, Indian Institute of Technology Bombay, Mumbai 400 076, India

E-mail: ankhi@phy.iitb.ac.in

Abstract. In this paper we report the efforts carried out to measure the branching ratio of $\eta \rightarrow \pi^0 \gamma \gamma$. The experiment was done using the tagged photon facility at ELSA, Bonn. A nearly full 4π set-up comprising of the Crystal Barrel and TAPS detector system was used. We describe the procedure followed to extract the branching ratio of this rare decay mode of eta. The simulations necessary to establish this procedure are presented first followed by data analysis.

Keywords. Rare eta-decay; chiral perturbation theory.

PACS Nos 14.40.Aq; 13.20.-v; 12.39.Fe

1. Introduction

The Standard Model for electroweak interaction has had tremendous success over the years. However, it can not be taken to be complete theory as it contains too many input parameters. It fails to answer some of the fundamental questions such as why we have three families of quarks and leptons. There is no explanation for CP violation or for the high spread in quark and lepton masses. There is no clue as to why we have left-handed doublets and right-handed singlets. It is thus clear that there is physics beyond the Standard Model. One way to probe this physics would be to probe the symmetries of the model such as C, CP and CPT.

The η meson provides an excellent test bed [1] for extending the validity of these symmetries. This is because all its possible strong decays are forbidden in the lowest order. The first-order electromagnetic decays are forbidden as well. The first allowed decay is the second-order electromagnetic transition $\eta \rightarrow \gamma \gamma$, with the result that the width of η is only 1.3 keV which is five orders of magnitude smaller than either the ρ or ω mesons.

The study of η mesons can also provide insight into one of the most successful existing theory of the strong and electroweak sector, the chiral perturbation theory (χ PTh). According to this theory, massless quarks come in two varieties, the left- and right-handed variety. The hadron dynamics is due to spontaneous breaking of chiral symmetry. To understand hadron dynamics one therefore needs to test the χ PTh. The reaction $\eta \rightarrow \pi^0 \gamma \gamma$ provides a gold-plated test for χ PTh. This decay is suppressed because of chiral symmetry of the L_0 term of L_{QCD} . In terms of momentum expansion used in χ PTh the leading $O(p^2)$ term is absent for massless

quarks and the $O(p^4)$ term is very small because there is no direct photon coupling to the π^0 and η . The order $O(p^4)$ term contributes only 3.9×10^{-3} eV. The first leading contribution therefore comes from $O(p^6)$ and hence provides a unique and stringent test of χ PTh up to order $O(p^6)$.

All the theoretical calculations for the width of this channel fall well below the experimental value listed by the PDG [2]. Moreover, the theoretical calculations based on χ PTh or the quark constituent models also do not agree amongst themselves as far as the decay of this channel is concerned.

A recent theoretical attempt by Oset *et al* [3] have predicted a width of 0.47 eV which is much larger than estimated by previous calculations based on χ PTh. In this study they have taken a coherent sum of VMD and chiral loops which enhances the decay width. They have also reasoned that the shape of the two-bachelor photons in this decay is crucially dependent on the number of contributing terms as shown in figure 1.

On the experimental front, again there is an inconsistency between two previous measurements, the GAMS-2000 and the Crystal Ball experiment. In GAMS-2000, $6 \times 10^5 \eta$ mesons were produced and decay photons were detected with GAMS 2000 spectrometer [2]. They have quoted a value of $(7.1 \pm 1.4) \times 10^{-4}$ for the branching ratio of this decay mode based on about 50 surviving events. In a subsequent effort, with the Crystal Ball detector which consists of 672 optically-isolated NaI(Tl) crystal, a total number of $3 \times 10^7 \eta$ mesons were produced [4]. They have calculated a width of 0.42 eV and a branching ratio of $(3.2 \pm 0.9) \times 10^{-4}$ for this channel. The importance of this channel therefore makes it imperative to resolve the inconsistency between the two measurements.

It is with this objective as well as to test the recent predictions by Oset *et al* [3] that we have undertaken to measure the branching ratio for the decay of this channel.

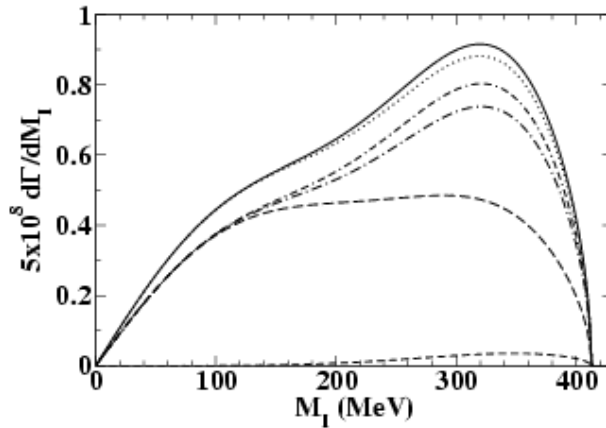


Figure 1. Contribution to the two-photon mass distribution. From bottom to top – short dashed line: chiral loops; long dashed line: only tree-level VMD; dashed-dotted line: coherent sum of the previous mechanisms; double dashed-dotted line: *idem* but adding the resummed VMD loops; continuous line: *idem* but adding the anomalous terms.

2. Experimental details

The experiment was performed at the Electron Stretcher Accelerator (ELSA) of Bonn. The ELSA was used to deliver a nearly continuous electron beam in the energy range 0.5 to 3.3 GeV. The electron beam then impinged on a radiator target to produce Bremsstrahlung photons. The electrons deflected by a magnet, fell on a tagging system which measured their energy. One thus has a tagged photon of energy $E_\gamma = E_0 - E_e^-$, where E_0 is the initial electron beam energy and E_e^- is the energy of the final scattered electron. This tagged photon hit a cylindrical liquid hydrogen target of 5 cm in length and 3 cm in diameter. The reaction products are detected in a detector system covering a nearly 4π solid angle and made up of the Crystal Barrel detector consisting of 1290 CsI(Tl) detectors and the TAPS detector which consists of 528 BaF₂ crystals. TAPS has been used as a forward wall. The target is surrounded by a three-layer scintillation fiber counter which returns one three dimensional spatial point for each charged particle traversing it. On the other hand, in front of each BaF₂ crystal we have VETO detector made up of plastic scintillator detector to identify charged and neutral hits. Energy and decay angle has to be determined with high resolution from both these detectors. TAPS detector has an additional feature that is, time information with high resolution. The charged hit was distinguished from the neutral hit if there was a signal either in scintillation fiber detector in front of Crystal Barrel detector or the VETO detectors in front of TAPS.

3. Analysis procedure

The channel that we are investigating is one of the rare decay modes of η and hence analysis procedure is involved. Extensive simulations have to be performed to understand the source of background. In the data, events having five particles in the final state were identified. To further correct the data, for finite energy and angular resolution of the detecting system, the procedure of kinematic fitting was adopted. In this section, we give a short description of the kinematic fitting, followed by simulations for the signal as well as noise. This help us to decide the cuts to be placed on the data to enhance the signal-to-noise ratio. Finally with the insight presented by simulations we present the analysis of the data done so far.

3.1 Kinematic fitting

This is a mathematical procedure in which one uses the physical laws governing a particle interaction or decay to improve the measurements of the process. Physical information is supplied via constraints. The analysis program then changes the vectors of the final state particles within the accepted angular and energy resolution of the detecting system so that one gets the minimum χ^2 for the constraints supplied.

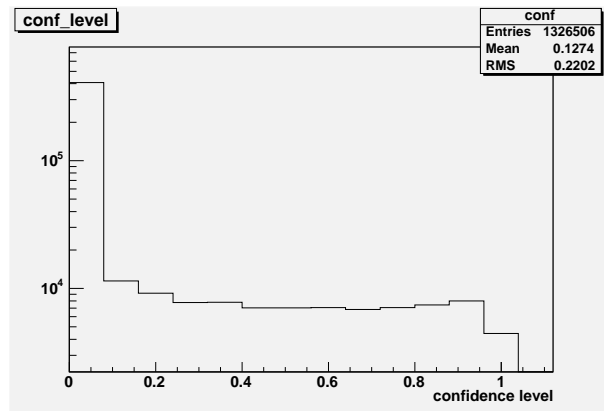


Figure 2. Confidence level plot.

We have used the following constraints in our analysis:

- momentum balance = 3,
- energy balance = 1,
- pion mass = 1,
- reaction-vertex = 1.

After performing the fit, one needs a way to check the agreement between data and hypothesis. Relevant quantity to make the judgment and decisions about the goodness of the fit is the confidence level. One can reduce the background by considering events for which the confidence level is flat. Figure 2 shows a typical confidence level plot for the data. One can see that beyond 0.1 the confidence level is flat. Therefore only events having a confidence level greater than 0.1 were analyzed.

One also has to make sure that the average change in the vectors of the final state particles should be zero. Pull is a normalized measure of the displacement of the measured values to the fitted values. A valid distribution of pulls will therefore form a normal distribution with width 1 and mean 0. Figure 3 shows a typical energy pull distribution of one of the final state particles. It was ensured that all the final state particles satisfied the requirements on the pull.

3.2 Simulation

As mentioned earlier detailed simulations help us in determining the cuts to be placed on the data so as to throw out maximum noise and minimum signal. The simulations have been done with the same conditions as experimental data. We have first performed the simulations for the signal followed by channels which could interfere with our signal.

Investigations of $\eta \rightarrow \pi^0\gamma\gamma$

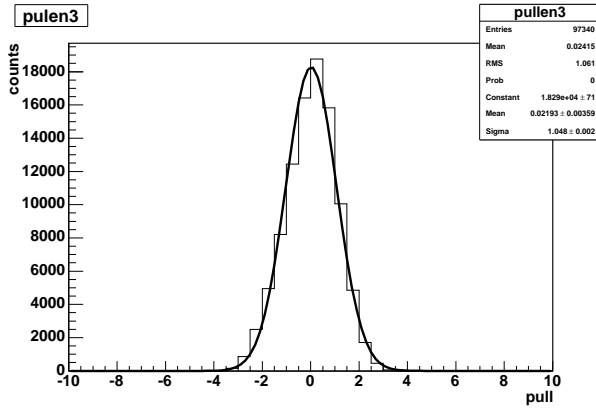


Figure 3. Pull of one final photon.

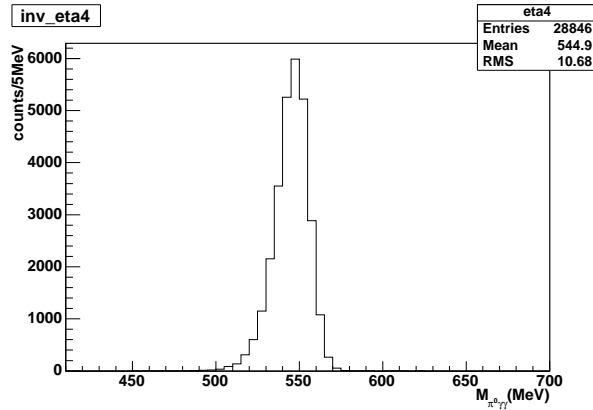


Figure 4. Signal of $\eta \rightarrow \pi^0\gamma\gamma$ decay channel from simulation.

3.2.1 $\eta \rightarrow \pi^0\gamma\gamma$

Figure 4 shows the signal of this channel. Out of the $20 \times 10^5 \eta$ incident on our detection system, we were able to construct $10 \times 10^5 \eta$. This roughly indicates that the efficiency of our system is about 50%. Figure 5 shows the vertex reconstruction of the η . As can be seen from the figure, the vertex is symmetrical about the center of the target.

We have performed the simulation of the following channels as background contributions.

1. $\omega \rightarrow \pi^0\pi^+\pi^-$,
2. $\eta \rightarrow \pi^0\pi^+\pi^-$,
3. $2\pi^0$,
4. $\eta \rightarrow 3\pi^0$.

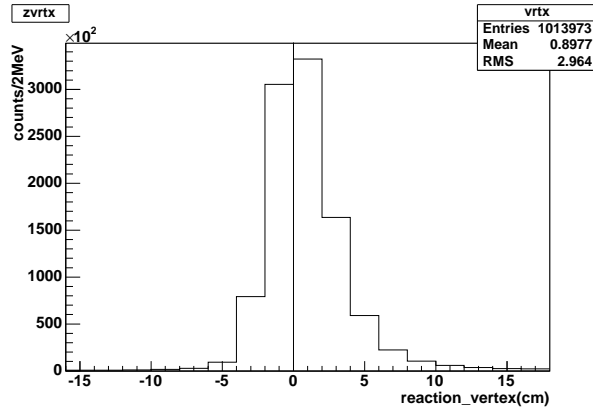


Figure 5. Reaction vertex of $\eta \rightarrow \pi^0\gamma\gamma$ from simulation.

Depending on simulations, we have applied different cuts to the data to remove the huge background.

3.2.2 $\omega \rightarrow \pi^0\pi^+\pi^-$

The efficiency of our detector system to remove charged events is not 100%. Thus a charged hit can be misidentified as a neutral hit. Hence, in such a situation $\omega \rightarrow \pi^0\pi^+\pi^-$ looks as $\pi^0\gamma\gamma$. This is the reason for considering this channel as a source of background. However, the huge contribution from this channel disappears by considering events having an incident energy less than 1 GeV. This is because the threshold for omega production is higher than 1 GeV and eta production goes down after 1 GeV incident beam energy.

3.2.3 $\eta \rightarrow \pi^0\pi^+\pi^-$

The reason of considering this channel as background is the same as we mentioned above in the case of the omega decay. Figure 6 shows the reaction-vertex plot of this background channel. The charged particles undergo multiple scattering and hence the reaction vertex is asymmetrical around zero as can be seen from figure 6. A cut on non-negative reaction vertex and incident beam energy less than 1 GeV, will considerably reduce the background coming from this channel.

3.2.4 $2\pi^0$

The reactions $\gamma + p \rightarrow p2\pi^0$ and $\eta \rightarrow \pi^0\gamma\gamma$ are kinetically identical. They produce the same number of particles in the final state and the cross-section for the former is orders of magnitude larger than the channel under investigation. The double π^0

Investigations of $\eta \rightarrow \pi^0\gamma\gamma$

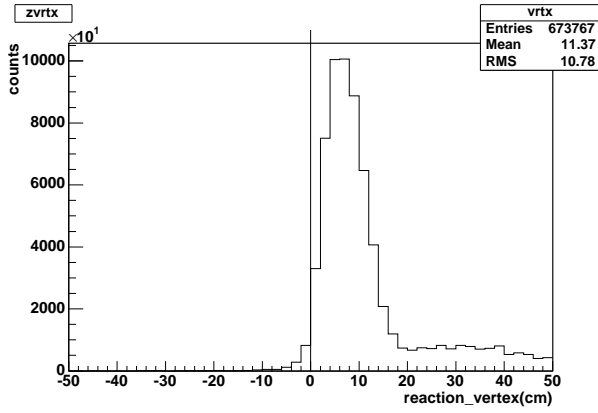


Figure 6. Reaction vertex of $\eta \rightarrow \pi^0\pi^+\pi^-$ background channel.

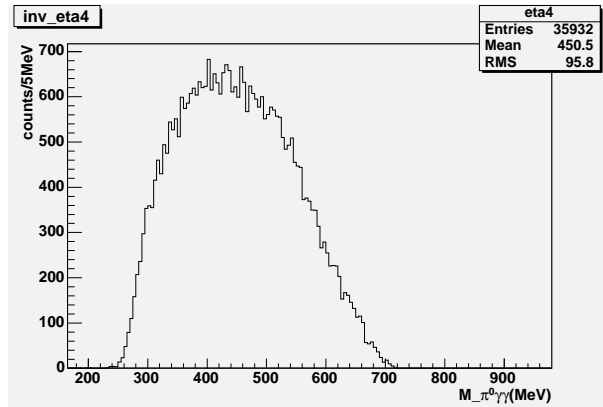


Figure 7. Background of $2\pi^0$ channel.

channel is therefore the main source of background in our study. Being identical in all respects, there is no way to remove this background by placing a cut on either incident beam energy or z -vertex. However, this background can not create a peak in the eta mass region. Figure 7 shows the invariant mass of this background channel.

3.2.5 $\eta \rightarrow 3\pi^0$

$\eta \rightarrow 3\pi^0$ channel has six photons in the final state. However, due to the inability of the detector system to identify two soft photons or merging of two photon clusters, events from this channel would look like a four-photon final state. Moreover, this background would also generate a small peak in the eta mass region. To make matters worse, the channel we are looking for is four orders of magnitude less than the $\eta \rightarrow 3\pi^0$ channel. One has to rely again on simulations to throw out noise due

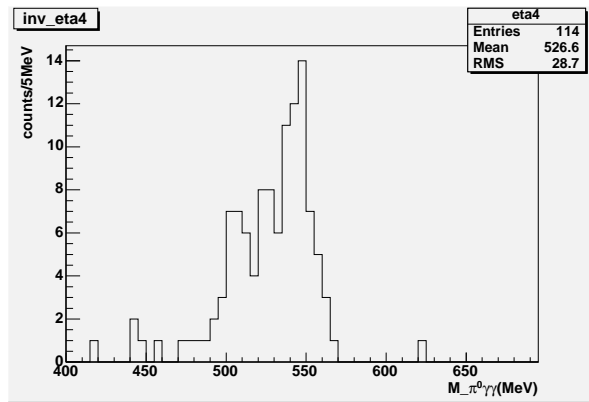


Figure 8. Background of eta decays into $3\pi^0$ channel.

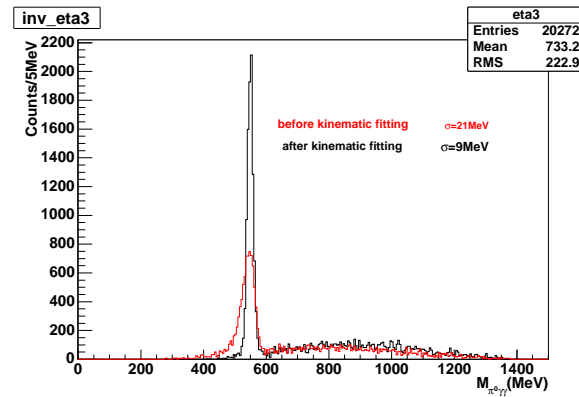


Figure 9. Eta decays into $3\pi^0$ before and after kinematic fitting.

to this channel. Figure 8 shows the invariant mass of this background channel. As can be seen there is contribution around η mass due to this channel.

3.3 Data analysis

Before analyzing the data, one has to be sure that the analysis procedure is working well. As the signal in our case is so weak, we cannot use it to test our computer codes. We therefore look at six-photon events in the final state which form η subsequently decaying into $3\pi^0$. We plot the invariant mass of the six photons before and after kinematic fitting. Figure 9 shows the invariant mass of $3\pi^0$ before and after kinematic fitting. The σ before the fit of the η as can be seen from the figure is 21 MeV whereas after fit it is only 9 MeV. The area under the peak are of the same order of magnitude for both. The important conclusion that we can draw from this is that by doing kinematic fitting we are neither removing counts from

Investigations of $\eta \rightarrow \pi^0\gamma\gamma$

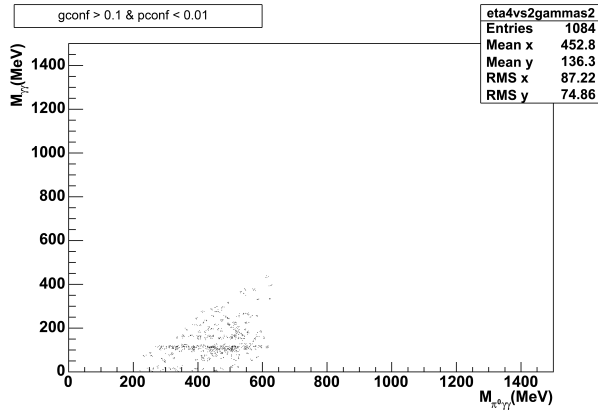


Figure 10. Invariant mass of $\pi^0\gamma\gamma$ vs $\gamma\gamma$.

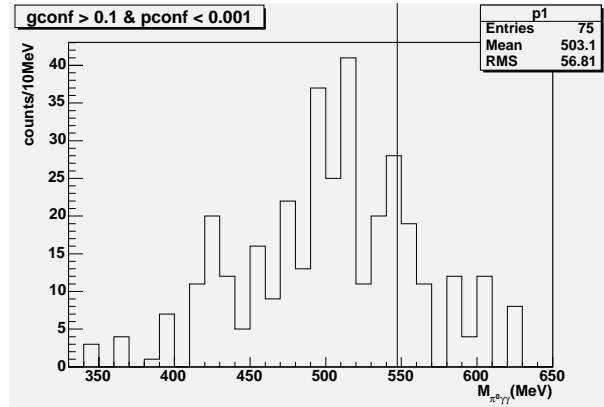


Figure 11. Projection of $\pi^0\gamma\gamma$.

the peak or putting counts in the peak. One can also conclude that using kinematic fitting we get a much better mass resolution.

We had applied fitting for double π^0 as well as $\eta \rightarrow \pi^0\gamma\gamma$ channel for five final state particles. All events where $\gamma + p \rightarrow p2\pi^0$ satisfies the confidence level greater than 0.001 were discarded from the analysis. Also we applied different cuts. They are incident beam energy cut and reaction vertex cut. The value of these cuts have been provided from the simulation studies mentioned earlier. Figure 10 shows the invariant mass of $\pi^0\gamma\gamma$ versus $\gamma\gamma$ plot.

To further remove events of the type $2\pi^0$ one can take a projection of figure 10 with a cut on the total energy of the bachelor photons such that the two do not form a pion. Figure 11 shows the projection of $\pi^0\gamma\gamma$ with invariant mass cut of $\gamma\gamma$ from 200 MeV to 400 MeV.

4. Conclusions

The analysis to calculate the branching ratio of $\eta \rightarrow \pi^0\gamma\gamma$ decay is underway from CBELSA/TAPS collaboration experiment. We expect better results because granularity of our detector system is better than the Crystal Ball detector. In addition, we have a fully determined final state. As can be seen from figure 11 there is some evidence of a small eta signal. These are just preliminary results. The data analysis is still in progress. From the branching ratio given in literature and with all cuts applied we expect about 200 events of the type $\eta \rightarrow \pi^0\gamma\gamma$ in our data. This we expect will help us to resolve the existing discrepancy between GAMS-2000 experiment and Crystal Ball data. In addition, the shape of the two-bachelor photons would in addition shed some light on the recent theoretical work [3]. In addition, we should get some estimate of $O(p^6)$ terms of the chiral perturbation theory.

References

- [1] B M K Nefkens and J W Price, *Phys. Scripta* **99(01)**, 114 (2002)
- [2] D Alde *et al*, *Z. Phys.* **C25**, 225 (1984)
- [3] E Oset *et al*, *Phys. Rev.* **D67**, 073013 (2003)
- [4] M Knecht *et al*, *Phys. Lett.* **B589**, 14 (2004)